ISBN: 978-3-95450-179-3 doi:10.18429/JACoW-FEL2017-MOP017

ECHO-ENABLED HARMONIC GENERATION RESULTS WITH ENERGY CHIRP

B. Garcia*, M.P. Dunning, C. Hast, E. Hemsing, T.O. Raubenheimer, SLAC, Menlo Park, USA
D. Xiang, Shanghai Jiao Tong University, Shanghai, China

Abstract

We report here on several experimental results from the NLCTA at SLAC involving chirped Echo-Enabled Harmonic Generation (EEHG) beams. We directly observe the sensitivity of the different n EEHG modes to a linear beam chirp. This differential sensitivity results in a multi-color EEHG signal which can be fine tuned through the EEHG parameters and beam chirp. We also generate a beam which, due to a timing delay between the two seed lasers, contains both regions of EEHG and High-Gain Harmonic Generation (HGHG) bunching. The two regions are clearly separated on the resulting radiation spectrum due to a linear energy chirp, and one can simultaneously monitor their sensitivities.

INTRODUCTION

There has long been an interest in producing fully coherent X-ray pulses in free electron laser facilities. One promising direction is to seed the electron beam with microbunching structure at the desired wavelength. Two popular methods to do this use either a single modulator-chicane combination, as in High-Gain Harmonic Generation (HGHG) [1] [2], or a dual modulator-chicane setup as in Echo-Enabled Harmonic Generation (EEHG) [3] [4].

We report here the results from a chirped electron beam with simultaneous regions of HGHG and EEHG bunching. The two regions are clearly distinguished by their central wavelength shift [5] and sensitivity to the chirp on the electron beam.

We also directly observe the sensitivity of the different $|n|$ EEHG modes to the linear chirp. By establishing an EEHG configuration with non-negligible and simultaneous bunching at multiple $|n|$ modes, we measure the sensitivity of these modes by observing their wavelength shift as a function of electron beam chirp.

Both of these setups generate a tunable, multi-color EEHG-seeded beam. These experiments were performed in 2015 at SLAC's NLCTA facility, concurrent with work towards producing an EEHG beam capable of radiating at the 75th harmonic of a 2400 nm seed laser [6].

THE NLCTA FACILITY

The electron beam at NLCTA is generated from a 1.6 cell BNL/ANL/UCLA/SLAC S-band (f = 2.856 GHz) photocathode gun and is boosted by two subsequent X-band (f = 11.424 GHz) accelerating structures to 120 MeV. At this point, the beam has a FWHM duration of ≈ 1 ps, a bunch charge of approximately 50 pC, and a small slice energy spread $\sigma_E \approx 1$ keV.

The beam then enters a modulating undulator (10 periods, λ_u = 3.3 cm, K = 1.82) where it interacts with an 800 nm (≈ 1 ps FWHM) laser. It then encounters a tunable four-dipole chicane before reaching a second modulating undulator (10 periods, λ_u = 5.5 cm, K = 2.76) where it interacts again with either a 800 nm or 2400 nm laser. The beam traverses a final magnetic chicane before being accelerated by a third X-band cavity which takes the energy to 160 − 192 MeV depending on the experiment. The beam finally enters a two-meter section of the VISA undulator [7] (100 periods, λ_u = 1.8 cm, K = 1.26) where any bunching produced by the upstream transformations is radiated as coherent radiation. This radiation is then diagnosed by a downstream EUV or VUV photon spectrometer [8].

SIMULTANEOUS EEHG AND HGHG SIGNALS

One difference between EEHG and HGHG signals is their response to a linear energy chirp. It has been shown that for the $n = -1$ EEHG mode and an HGHG configuration at the same target harmonic, the central wavelength of the HGHG setup is more sensitive to electron beam chirp then EEHG [5] [9]. This provides a powerful way of discriminating between EEHG and HGHG signals should both be present on the same electron beam.

In HGHG a single modulator produces a sinusoidal energy modulation of magnitude ΔE and at wavenumber k_1 which is converted into a density modulation by a chicane with longitudinal dispersion R_{56}. The resulting bunching is significant at integer harmonics of the laser wavenumber $k = ak_1$ and is [2],

$$b_a^{\mathrm{HGHG}} = \left| e^{-\frac{1}{2}(B_1^2 a^2)} J_h(-aA_1B_1) \right|, \quad (1)$$

where $A_1 = \Delta E_1/\sigma_E$, $B_1 = R_{56}^{(1)} k_1 \sigma_E / E_0$. Notably, in order to increase the bunching at a higher harmonic, one must increase the modulation amplitude A_1 and hence the induced energy spread.

In EEHG, there are two chicanes and two separate laser modulators with possibly different laser wavenumbers and the relation $\kappa = k_2/k_1$. This process produces bunching at wavenumbers $k_{n,m} = nk_1 + mk_2$ which is given by [3],

$$b_{n,m} = \left| e^{-\frac{1}{2}(nB_1 + aB_2)^2} J_n(nB_1 + aB_2) J_m(-aA_2B_2) \right|, \quad (2)$$

where $a = n + m\kappa$. Analysis of this bunching spectrum reveals that the $n = -1$ harmonics can achieve the most significant bunching. The finely-spaced energy bands created

* bryantg@stanford.edu

ISBN: 978-3-95450-179-3 doi:10.18429/JACoW-FEL2017-MOP017

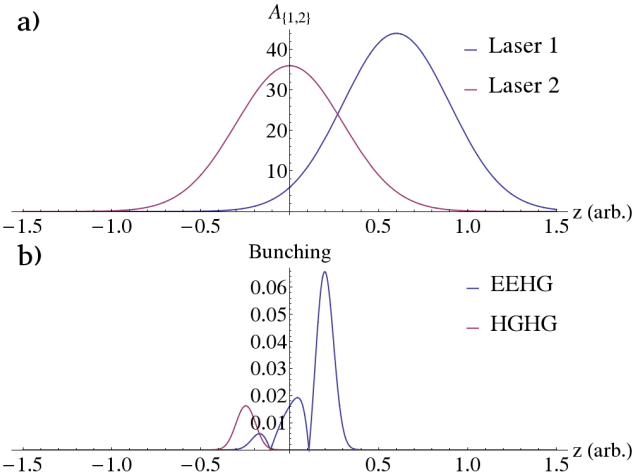

Figure 1: The EEHG and HGHG signals for Gaussian, temporally offset laser beams. Fig. a) shows the laser profiles, each of which is a Gaussian with $\sigma_z = 0.3$. Fig. b) shows the resulting bunching, both due to EEHG and HGHG showing clearly separated regions.

by the large first chicane in EEHG also allow high harmonics to be obtained with modest laser modulation amplitudes when compared with HGHG.

In order to generate a beam with both EEHG and HGHG signals, the temporal delay between the first and second modulation lasers can be adjusted. Due to this delay, there may exist a region of significant overlap between the two modulations, but also regions in which only the second laser is significant. This can create distinct regions in which the EEHG process is effective, and others in which the HGHG contribution dominates.

Since the usual definition of the bunching factor is global in nature, we instead use the notion of a local bunching factor defined as,

$$b(k, z_0, \delta_z) = \frac{1}{N_{e,z}} \left| \sum_{i=1}^{N_{e,z}} e^{ikz_i} \right|_{|z_0 - z_i| < \delta z}, \qquad (3)$$

where k is the wavenumber of interest and we are interested in a longitudinal region of size δ_z centered around the position z_0 which contains $N_{e,z}$ particles. This definition allows us to speak of a longitudinal position-dependent bunching factor, and identify the distinct regions of bunching.

We can employ the previous bunching analyses of Eqns. 1 and 2 by promoting the laser modulation amplitudes to local quantities: $A_{1,2} \rightarrow A_{1,2}(z)$, where $z = s - \beta ct$ is the intra-bunch longitudinal coordinate. Some care should be taken in interpreting this resulting bunching factor, as it assumes that the each individual subsegment at location z is infinite in longitudinal extent. However, as long as one is not concerned with the bandwidth of the resulting signals, and the typical length scale of change for $A_{1,2}(z)$ is significantly longer than the radiation wavelength it remains a reasonable approximation to consider.

To model the effect we consider a longitudinally infinite electron beam modulated by two lasers which are both Gaussian in temporal extent with scaled length $\sigma_z = 0.3$. The peak modulation amplitudes are $A_1 = 44$ and $A_2 = 36$, and the centers are offset by a scaled distance of $\Delta z = 0.6$. These laser profiles are shown in Fig. 1 a). The scaled dispersions are set to $B_1 = 0.818$ and $B_2 = 0.13$. The resulting bunching spectrum, both due to EEHG and HGHG contributions, is shown in Fig. 1 b). The bunching is computed assuming a laser wavenumber ratio $\kappa = 1/3$ and $n = -1$, $m = 21$.

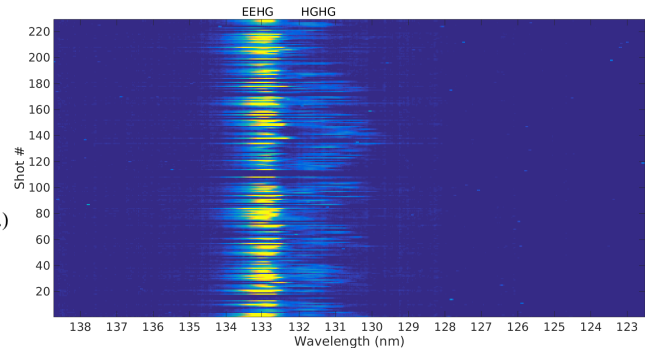

Figure 2: Simultaneous EEHG and HGHG signals in the vicinity of 133 nm. Both signals represent the 18th harmonic of the 2400 nm seed laser.

In the region of significant laser overlap, a strong EEHG signal is established. However, in the region $z \approx -0.4$ only the second laser is relevant and this allows a pure HGHG signal to exist in there.

This situation was approximately recreated at the NLCTA with a final beam energy of $E \approx 184$ MeV and using two lasers of wavelengths $\lambda_1 = 800$ nm and $\lambda_2 = 2400$ nm. An EEHG signal was established in the neighborhood of the 18th harmonic, or 133 nm, and then the lasers de-tuned in time to create the distinct regions of bunching. The resulting spectrum across 220 separate shots (≈ 22 seconds) is shown in Fig. 2. The chicanes were set to $R_{56}^{(1)} = 12.5$ mm and $R_{56}^{(2)} = 2$ mm to give $B_1 = 0.818$ and $B_2 = 0.130$.

The magnitude of the linear chirp can be quantified by scaled parameter $h_1 = \frac{1}{k_1} \frac{dp_0}{dz}|_{z=0}$ [9]. The separation in wavelengths due to this linear chirp ($h_1 \approx -0.144$ from HGHG, $h_1 \approx 1.18$ from EEHG) imparted to the electron beam prior to modulation in one of the accelerating structures. Note the differing signs of h_1 imply that the EEHG and HGHG signals were established on the oppositely chirped sides of the electron beam. Due to the particular EEHG configuration, however, both harmonics blue shift in the presence of these chirps.

This observation is similar to the EEHG and HGHG plots shown in [10], and is an extension into the high-harmonic regime of the initial HGHG/EEHG results [11]. This result suggests the possibility of manipulating the modulation envelopes of the lasers to create and control distinct areas of bunching for potential use in multi-color FEL applications.

MULTI-COLOR EEHG EFFECTS

Multi-color operation modes are possible not only in a mixed HGHG-EEHG beam configuration, but also within

ISBN: 978-3-95450-179-3 doi:10.18429/JACoW-FEL2017-MOP017

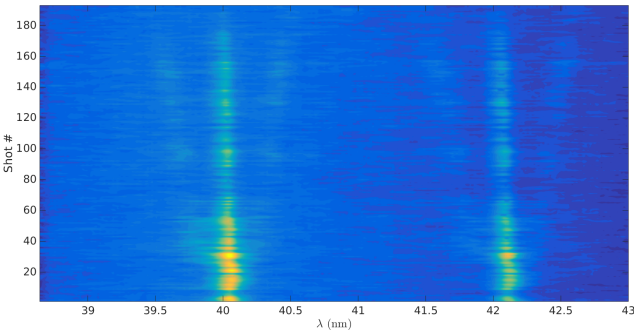

Figure 3: The splitting of the main echo peaks due to an increase in linear chirp. The shot number is correlated with RF phase increase such that the difference between shot 0 and 200 is approximately 15 degrees in RF phase (for the first RF structure).

one which is purely EEHG. This possibility again comes about due to the sensitivity to linear energy chirp on the electron beam. This linear chirp has the effect of shifting the echo harmonic a for a given echo configuration to the location [5],

$$a' = \frac{n + m\kappa(1 + h_1 B_1)}{1 + h_1 B_1}. \tag{4}$$

This central wavelength shift is dependent on the particular mode numbers n, m. We therefore conclude that EEHG configurations with different values for $|n|$, although nominally at the same wavelength for $h_1 = 0$, will not overlap in the case of nonzero electron beam chirp. In particular, for a mode with n offset Δn,

$$a(n + \Delta n) = a(n) - \Delta n \frac{h_1 B_1}{1 + h_1 B_1}. \tag{5}$$

It is possible to choose EEHG parameters such that there exists significant simultaneous bunching due to multiple n modes. As an electron beam chirp is applied, these initially degenerate modes will split into several sub-peaks depending on the magnitude of chirp and which $|n|$ modes are excited.

To test this idea at NLCTA, we used an EEHG configuration with 800nm/800nm lasers and tuned the configuration for Echo-20 at 40 nm. The dispersions were set as $R_{56}^{(1)} = 12.5$ mm and $R_{56}^{(2)} \approx 0.57$ mm, and the final beam energy for was 162 MeV. The RF phase in the first accelerating structure, which provides an approximate 60 MeV energy boost, was adjusted by approximately 15 degrees of phase over the course of 20 seconds, or 200 shots. The resulting spectrum in the vicinity of 40 nm is shown in Fig. 3.

Comparing the shift in the central wavelength of the $n = -1$ harmonic and Eqn. 4 gives $h_1 B_1 \approx 0.27$ by around the 170th shot. The in the shift of the $n = -1$ mode implies a positive electron beam chirp ($h_1 > 0$) for these EEHG parameters, although an optimal configuration with higher B_1 would respond oppositely to the same chirp [9].

We observe that as the RF phase is increased, two distinct sidebands form and move away from the central $n = -1$ peak. Numerical simulations of this EEHG setup show that the approximate maximum for the $n = -1, m = 21$ echo bunching of $\approx 7.5\%$ is given when $A_1 \approx 25$ and $A_2 \approx 31$, which is consistent with the measured values of the laser modulations. In this configuration, there is nonzero bunching in the $n = -2, m = 22$ and $n = 0, m = 20$ modes at approximately the 1-2% level, while all other modes have bunching at $< 0.1\%$ and are not visible. From Eqn. 5, the $n = 0$ and $n = -2$ modes shift with opposite sign and equal magnitude away from the central peak, which gives rise to the equally spaced sidebands visible in Fig. 3. The magnitude of these shifts are consistent with the determination of $h_1 B_1 = 0.27$ from the central peak.

In this particular configuration, the magnitude of the sideband bunchings are approximately equal, however this need not be the case. For example, choosing instead $A_2 = 34$ leaves a non-negligible subsidiary bunching factor only in the $n = -2$ and $n = -1$ modes which would result in an asymmetric sideband spectrum.

DISCUSSION

The techniques demonstrated here both rely on a chirped electron beam which is then seeded via EEHG. Multicolor signals can be produced either through the simultaneous production of regions of EEHG and HGHG bunching, or through the generation of significant bunching at multiple $|n|$ modes.

While the techniques demonstrated here merely generated multi-color coherent emission, ultimately one would like to seed an FEL. In order to amplify multiple colors in an FEL the separate colors must be separated from the resonant wavelength by $\Delta\lambda/\lambda \lesssim \rho$. To take a numerical example, consider an EEHG-seeded EUV FEL with $\rho = 10^{-3}$, $\sigma_E = 100$ keV, and lasers with $\lambda_1 = \lambda_2 = 266$ nm operating at the 50th harmonic (5.32 nm). Full control of the $n = -1$ optimized wavelength within the FEL bandwidth could be obtained by a zero-crossing X-band cavity with power to provide a 100 MeV on-crest increase in beam energy.

It therefore seems plausible that the electron beam chirp could be used to create tunable, multi-color pulses at a full FEL facility. Dedicated studies with a zero-crossing RF cavity would provide an excellent test bed to examine in more depth the effects presented in this paper.

ACKNOWLEDGMENTS

This work was supported in part by the U.S. Department of Energy under Contract No. DE-AC03-76SF00515 and the Stanford University Bob Siemann Fellowship in Accelerator Physics.

REFERENCES

[1] I. Ben-Zvi *et al.*, "Proposed uv fel user facility at bnl," *Nuclear Instruments and Methods in Physics Research Section A: Accelerators, Spectrometers, Detectors and Associated Equipment*, vol. 304, no. 1, pp. 181 – 186, 1991. [Online]. Available: http://www.sciencedirect.com/science/article/pii/016890029190845H

ISBN: 978-3-95450-179-3 doi:10.18429/JACoW-FEL2017-MOP017

[2] L. H. Yu, "Generation of intense uv radiation by subharmonically seeded single-pass free-electron lasers," *Phys. Rev. A*, vol. 44, pp. 5178–5193, Oct 1991. [Online]. Available: http://link.aps.org/doi/10.1103/PhysRevA.44.5178

[3] G. Stupakov, "Using the beam-echo effect for generation of short-wavelength radiation," *Phys. Rev. Lett.*, vol. 102, p. 074801, Feb 2009. [Online]. Available: http://link.aps.org/doi/10.1103/PhysRevLett.102.074801

[4] D. Xiang and G. Stupakov, "Echo-enabled harmonic generation free electron laser," *Phys. Rev. ST Accel. Beams*, vol. 12, p. 030702, Mar 2009. [Online]. Available: http://link.aps.org/doi/10.1103/PhysRevSTAB.12.030702

[5] Z. Huang *et al.*, "Effects of energy chirp on echo-enabled harmonic generation free-electron lasers," in *Proceedings of the 31st International Free Electron Laser Conference (FEL 09), Liverpool, UK*, STFC Daresbury Laboratory, 2009.

[6] E. Hemsing *et al.*, "Echo-enabled harmonics up to the 75th order from precisely tailored electron beams," *Nature Photonics*, 2016.

[7] R. Carr *et al.*, "Visible-infrared self-amplified spontaneous emission amplifier free electron laser undulator," *Phys. Rev. ST Accel. Beams*, vol. 4, p. 122402, Dec 2001. [Online]. Available: http://link.aps.org/doi/10.1103/PhysRevSTAB.4.122402

[8] B. Garcia *et al.*, "Facility upgrades for the high harmonic echo program at slac's nlcta," in *Proceedings of the 2015 FEL Conference*, Daejeon, Korea, 2015.

[9] E. Hemsing *et al.*, "Sensitivity of echo enabled harmonic generation to sinusoidal electron beam energy structure," *Phys. Rev. Accel. Beams*, vol. 20, p. 060702, Jun 2017. [Online]. Available: https://link.aps.org/doi/10.1103/PhysRevAccelBeams.20.060702

[10] E. Hemsing *et al.*, "Highly coherent vacuum ultraviolet radiation at the 15th harmonic with echo-enabled harmonic generation technique," *Phys. Rev. ST Accel. Beams*, vol. 17, p. 070702, Jul 2014. [Online]. Available: http://link.aps.org/doi/10.1103/PhysRevSTAB.17.070702

[11] D. Xiang *et al.*, "Demonstration of the echo-enabled harmonic generation technique for short-wavelength seeded free electron lasers," *Phys. Rev. Lett.*, vol. 105, p. 114801, Sep 2010. [Online]. Available: http://link.aps.org/doi/10.1103/PhysRevLett.105.114801